

Supplementary Information

Novel Photocatalytic Antibacterial Activity of TiO₂ Microspheres Exposing 100% Reactive {111} Facets

Liang Sun,^a Ying Qin,^b Qingqing Cao,^a Bingqing Hu,^a Zhiwei Huang,^a Ling Ye^{*b} and Xingfu Tang^{*a}

^a Department of Environmental Science and Engineering, Fudan University, Shanghai, 200433, China; E-mail: tangxf@fudan.edu.cn; Fax: +86 21 6564 3597

^b School of Chemical Biology and Pharmaceutical Sciences, Capital Medical University, Beijing 100069, China; E-mail: lingye@ccmu.edu.cn

1. Experimental Section

1.1. Material Preparation

An aqueous solution (50 mL) containing titanium trichloride (TiCl₃, 0.15 M) and sodium chloride (NaCl, 3 M) was initially sealed in a *p*-polyphenylene-lined autoclave, and then heated at 200 °C in an oven for 16 h. The obtained precipitation was filtered, washed and dried at 110 °C overnight, followed by calcined at 400 °C in air for 4 h to obtain the TiO₂ microspheres.

1.2. Structure Characterization

X-ray powder diffraction (XRD) patterns were recorded with a D8 Advance diffractometer using nickel-filtered Cu K_α ($\lambda = 0.15418$ nm) radiation. Morphologies of the samples were investigated by scanning electron microscopy (SEM, Philips XL30), and detailed structures were examined both with field-emission scanning electron microscopy (FE-SEM, Hitachi S-4800) and high resolution field-emission transmission electron microscopy (TEM & HRTEM, JEOL JEM 2100F). Nitrogen adsorption-desorption isotherms and specific extrasurface area of the TiO₂ samples were obtained at –196 °C using a Micromeritics Tristar ASAP 3000 instrument.

1.3. Analyses of Hydroxyl Radical ($\cdot\text{OH}$)

The concentrations of the $\cdot\text{OH}$ generated from the UV illuminated TiO_2 surfaces were measured using a terephthalic acid (TA) fluorescence probe method. The terephthalic acid (TA) was used as a fluorescence probe. The typical procedure was as follows: 0.01 g of the TiO_2 sample (microspheres or Degussa P25) was dispersed in a base aqueous solution (50 mL, TA = 5×10^{-4} M, and NaOH = 2×10^{-3} M) to form a suspension. The suspension was subjected to ultrasonic dispersion for 10 min in dark and then divided into eight equal aliquots (3 mL) for UV light irradiation with different irradiation time (energy output = 4 W, major wavelength = 365 nm, Philips black light lamp). The average light intensity striking on the surface of the suspension was *ca.* 350 $\mu\text{W}/\text{cm}^2$. After the TiO_2 sample was separated from the solution through filtration, the residual limpid mother solution was used for fluorescence spectrum measurements. Fluorescence spectra were recorded on a Hitachi F-2500 FL fluorescence spectrophotometer using the 315 nm excitation light.

1.4. Confocal Microscope Analysis of Reactive Oxygen Species (ROS)

Reactive oxygen species (ROS) (mainly $\cdot\text{OH}$) produced from the TiO_2 microspheres under UV light irradiation were visualized using confocal laser scanning microscope (CLSM) with 2,7-dichlorodihydrofluorescein (DCFH) as a fluorescence probe molecule. Due to the high self-oxidizability of DCFH for long restore time, the stable DCFH diacetate form (DCFH-DA) was used as the starting material. DCFH-DA can be converted to DCFH by NaOH hydrolysis. The fluorescence probe solution was prepared as follows, 0.5 mL of 1 mM DCFH-DA ethanol solution was dispersed in 2 mL 0.01 M NaOH aqueous solution and allowed to stand in dark for 30 min to generate DCFH. Then, the above mixture was diluted to 5 μM with 0.1 M PBS buffer to obtain the final fluorescence probe solution. The TiO_2 microspheres were dispersing in above solution to form 50 $\mu\text{g}/\text{mL}$ suspension. One drop taken from above suspension was dripped on a glass sheet and exposed to the irradiation for 20 min (the irradiation condition was the same as introduced in the Analysis of $\cdot\text{OH}$ Section). After irradiation, the

glass sheet was immediately mounted for imaging analysis on a Leica TCS SP5 CLSM with the excitation light at 488 nm.

1.5. Photocatalytic Antibacterial Experiment

All the reagents and apparatus were after autoclaved sterilization process before used in antibacterial experiment. Desired amount of the TiO₂ microspheres were dispersed in 20 mL deionized water to form the suspension, and then filtered with a 25 mm diameter cellulose acetate membrane filter holder with an average pore size of 0.22 µm, followed by filtration of 10 mL *Staphylococcus Aureus* (*S. aureus*) suspension (1×10^4 CFU/ml) onto the TiO₂-loaded filters. For the blank group, 10 mL of the bacterial suspension was filtered through a TiO₂-uncoated filter. Each filter was then put on an empty sterile Petri dish. The sterile Petri dishes were placed in a biochemical incubator with temperature at 37.0 °C. For the photocatalytic experiment, all samples received photo irradiation for 2 h from a Philips black lamp (energy output = 8 W, major wavelength = 365 nm). The average light intensity striking on the surface of the Petri dish was controlled at *ca.* 100 µW/cm². After photo irradiation, the filters were immediately removed from the Petri dishes, eluted with PBS buffer, and the eluent was then transferred onto LB agar plates. The plates were allowed to grow for 24 h at 37.0 °C before counted for viable bacteria. The viable bacteria was monitored by counting the number of colony-forming units from the appropriate dilution on culture medium. The survival rate (*S*) was calculated as follows: $S = \frac{N}{N_u}$, where *N* was the number of CFUs after irradiation of the TiO₂-coated test samples and *N_u* was the number of CFUs after irradiation of the blank sample.

For rutile TiO₂ microsphere, the amount of sample used in each group was determined by assuming that each microsphere had a regular spherical shape with diameter of 2 µm, so each sphere could be considered as a cube with a 2 µm edge length. After filtered cellulose acetate membrane filter holder, the cubes were assumed to uniformly distribute on the filter to form layer. Here the 0.5, 1.0, 1.5 and 2.0 layers were chosen to test antibacterial activity. The mass amount of the TiO₂ microspheres was obtained through multiplying total volume of cubes by specific gravity (4.23 g/cm³) of rutile TiO₂. For comparison,

the amount of test P25 was determined by ensuring that the total external surface area of P25 was equal to the corresponding microspheres (extrasurface area of microspheres and P25 are $4.9\text{ m}^2/\text{g}$ and $41.4\text{ m}^2/\text{g}$, respectively).

2. Results and Discussion

2.1. Isothermal Adsorption/Desorption Curves and Pore-Size Distribution of the Microspheres

The N_2 adsorption-desorption isotherms and the corresponding pore size distributions of the TiO_2 microspheres are shown in Fig. S1. The isotherms recorded for the microspheres correspond to the Type IV adsorption isotherms, characteristic of the mesoporous or macroporous solid, and a hysteresis loop of Type H3 for the microsphere occurs at the high p/p_0 , suggesting the existence of slit-shaped capillaries with parallel plates.¹ The pore size distribution is calculated by the BJH model. Obviously, the pore sizes of the microspheres are predominantly in a wide range of 25–75 nm, with one strong peak around 45 nm and another at 100 nm, possibly indicative of the presence of the funnel shaped pore.

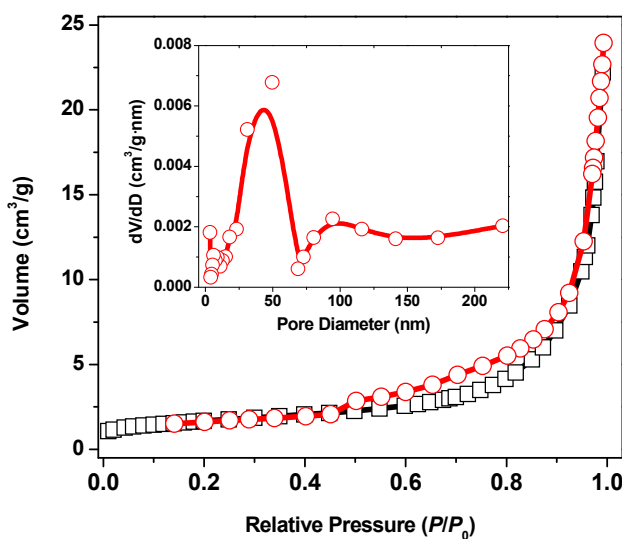


Fig. S1 N_2 adsorption–desorption isotherms and corresponding pore-size distribution curves of the microspheres.

2.2. Filling Rate Evaluation of the Rutile TiO_2 Spherical Faces

The filling rate (R_f) in terms of the summed section areas of the nanorod ends to the spherical surface of the rutile TiO_2 spherical faces was evaluated using a software of Adobe Photoshop CS2. The center part of one typical microsphere was selected for R_f evaluation to eliminate the error due to the viewing

angle, as shown in Fig. S2a. The areas of slight dark color in Fig. S2b, which can be colored green using the magic wand tool of the Adobe Photoshop CS2 (Fig. S2c), is due to the interstice between the nanorods and the one with light color due to the nanorod tops, and thus the value of R_f can be calculated to approximately 83% via the pixel ratio of the grey to the grey + green one (Fig. S2c).

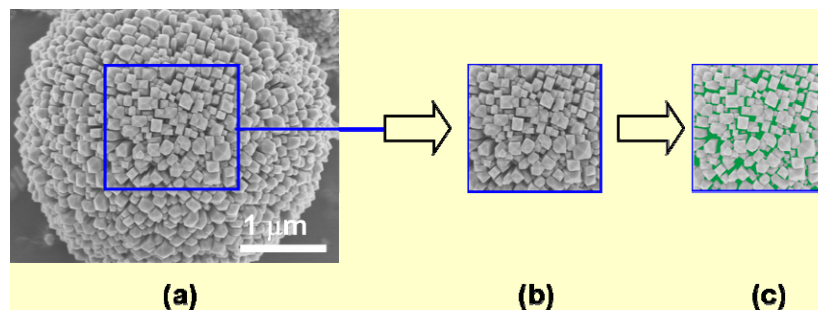


Fig. S2 Calculated filling rate of the nanorods on the rutile TiO₂ spherical surface.

2.3. Projected Angle Calculation of the HRTEM Image

Fig. S3a displays the structure model of the nanorod top. In order to determine the θ' angle in Fig. S3b, we suppose that the coordinates of point A, B, C, D and P would be indexed as (a,0,0), (0,a,0), (-a,0,0), (0,-a,0) and (0,0,c), respectively, where a and c represent the lattice parameters ($a = 0.45927$ nm, $c = 0.29544$ nm) of rutile TiO₂ crystal calculated from the XRD pattern (Fig. 1a). Thus, it is easy to establish the corresponding relationship between the planes in Fig. S3 and the crystal facets of the rutile TiO₂. For example, the PBA and PBC are planes (111) and (-111) facets, respectively.

As shown in Fig. S3a, the value of θ ($\theta = 32.75^\circ$) in the given triangle APO (Δ APO) can be calculated from the following formula (1).

$$\operatorname{tg} \theta = \frac{OP}{OA} = \frac{c}{a} = \frac{0.29544}{0.45927} = 0.6433 \quad (1)$$

The θ' angle is given by projecting the Δ APO on the (1-20) plane, and obviously the θ' is the projected angle of the θ on the (1-20) plane, as shown in Fig. S3c, which can be calculated to be 35.72° ($\theta' = 35.72^\circ$) according to the formula (2).

$$\operatorname{tg} \theta' = \frac{OP}{OA'} = \frac{OP}{OA \cdot \cos \alpha} = \frac{c}{a \cdot \cos \alpha} = 0.7192 \quad (2)$$

where $a = 0.45927$ nm, $c = 0.29544$ nm and α is the intersection angle between the (010) plane (Δ APO) and the (1-20) plane which is calculated to be 26.56° from the crystal structure and the values of both a and c . The value of θ' is close to the corresponding measured value (*ca.* 36°) between the side line and the (001) plane in Fig. 2c, strongly suggesting that the tops of the tetragonal prism TiO₂ nanorods are enclosed by the {111} facets.

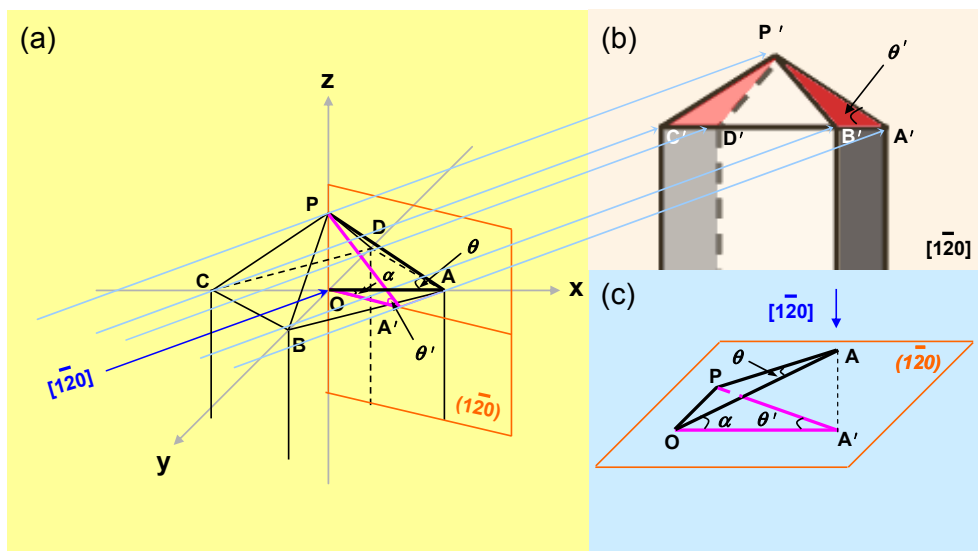


Fig. S3 Structure analysis of the nanorod top viewed in TEM images.

2.4. Exposed {111} Facet Areas on the TiO₂ Spherical Surface

To calculate the summed surface area of {111} facets on one rutile TiO₂ microsphere, a tetragonal pyramid on nanorod top and the corresponding schematic model are shown in Fig. S4. Therefore, the spherical surface area of the rutile TiO₂ microsphere (S_{sphere}) can be calculated from the formula (3):

$$S_{sphere} = 4 \cdot \pi \cdot r^2 = 12.6 \mu\text{m}^2 \quad (3)$$

where $\pi = 3.14$ and $r = 1.0 \mu\text{m}$, the average radius of the rutile TiO₂ microspheres.

As the structure model of the nanorod displayed in Fig. S4, the area of the ABCD curved surface ($S_{curved\ surface} \approx 4.90 \times 10^{-3} \mu\text{m}^2$) can be calculated according to the formula (4) and using a software of the Matlab 6.5, approaching to the area ($S_{square} = d^2 = 70 \text{ nm} \times 70 \text{ nm} = 4.90 \times 10^{-3} \mu\text{m}^2$) of the ABCD plane ($S_{curved\ surface} \approx S_{square}$)

$$S_{\text{curved surface}} = \iint \frac{r^2}{\sqrt{r^2 - x^2 - y^2}} dx dy, \left(-\frac{d}{2} \leq x \leq \frac{d}{2}, -\frac{d}{2} \leq y \leq \frac{d}{2} \right) \quad (4)$$

where $r = 1.0 \mu\text{m}$, the average radius of the rutile TiO_2 microspheres, and $d = 70 \text{ nm}$, the average width of the nanorods. Thus, the total areas ($S_{\text{CURVED SURFACE}}$) of all curved surface of the **WHOLE** sphere is $10.5 \mu\text{m}^2$ ($S_{\text{CURVED SURFACE}} = S_{\text{sphere}} \times R_f$), and the total areas ($S_{\text{total}\{111\}}$) of the $\{111\}$ facets of one **WHOLE** TiO_2 microsphere may be calculated as the following formula (5) because the total S_{square} equals $S_{\text{CURVED SURFACE}}$.

$$S_{\text{total}\{111\}} = \frac{S_{\text{CURVED SURFACE}}}{\cos \beta} = 14.2 \mu\text{m}^2 = 113\% S_{\text{sphere}} \quad (5)$$

where $\beta = 42.3^\circ$, the intersecting angle between the (001) plane and the (111) one, as shown in Fig. S4. Clearly, $S_{\text{total}\{111\}}$ is larger than the S_{sphere} .

Therefore, the TOTAL area of the exposed $\{111\}$ facets on one rutile TiO_2 microsphere is 113% as the spherical surface area of the WHOLE microsphere ($S_{\text{total}\{111\}} = 113\% S_{\text{sphere}}$).

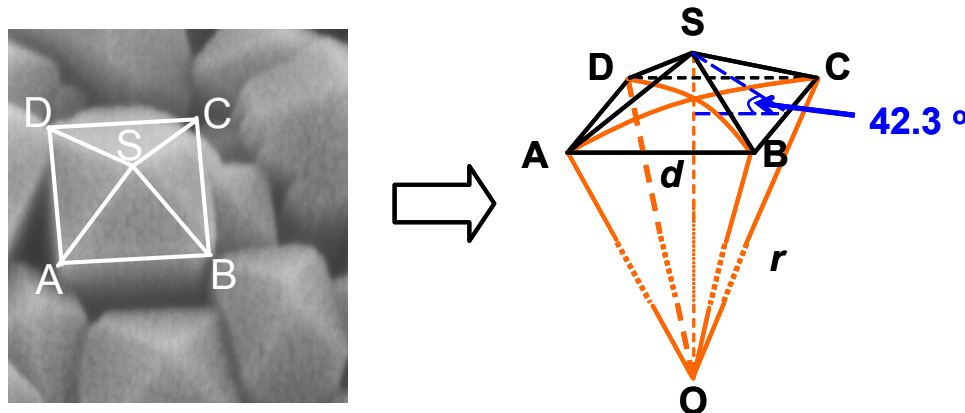


Fig. S4 Top SEM image and structure model of the nanorod top.

2.5. XRD Pattern and SEM Image of P25

The Degussa P25 TiO_2 used here has a crystal distribution of 82% anatase and 18% rutile determined from the XRD pattern displayed in Fig. S5a. The P25 nanoparticles also have irregular-shaped morphologies with mean size of *ca.* 30 nm (Fig. S5b).

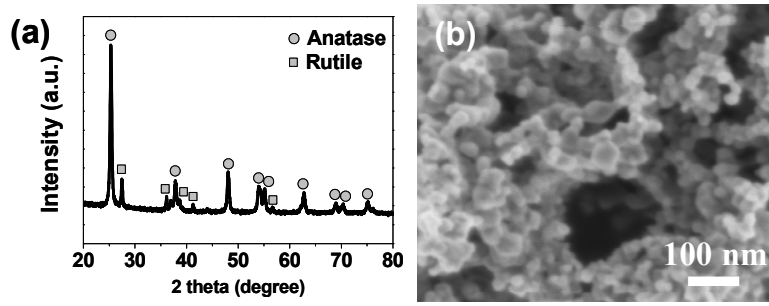


Fig. S5 XRD pattern (a) and FE-SEM image (b) of P25 TiO₂.

2.6. Analyses of Hydroxyl Radical (\cdot OH)

The efficiency for photocatalytic reaction of rutile TiO₂ microspheres or P25 was determined by monitoring the formation of active \cdot OH upon UV irradiation because \cdot OH radicals are considered as the most important oxidative specie in photocatalysis reactions. TA was used as a fluorescence probe as it could readily react with \cdot OH to produce the highly fluorescence emitting product, 2-hydroxy terephthalic acid (TAOH), with unique fluorescence signal featuring a peak around 425 nm. The intensity of this fluorescence peak at 425 nm is in proportion to the amount of \cdot OH radicals produced in water.² Fluorescence emission spectra associated with TAOH was generated upon irradiation with different time are shown in Fig. S6.

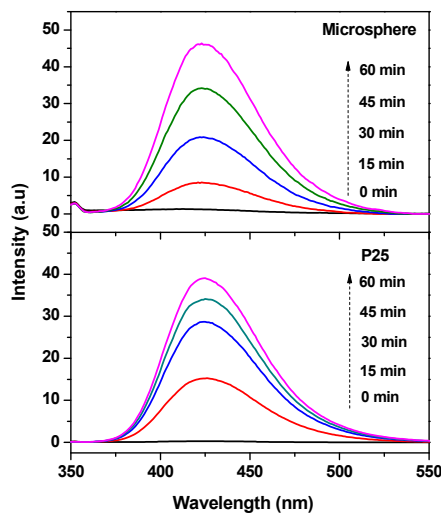


Fig. S6 Fluorescence emission spectra of TiO₂ in the presence of TA (0.5 mM) with different irradiation time.

2.7. Photocatalytic Antibacterial Performances of the Microspheres and P25

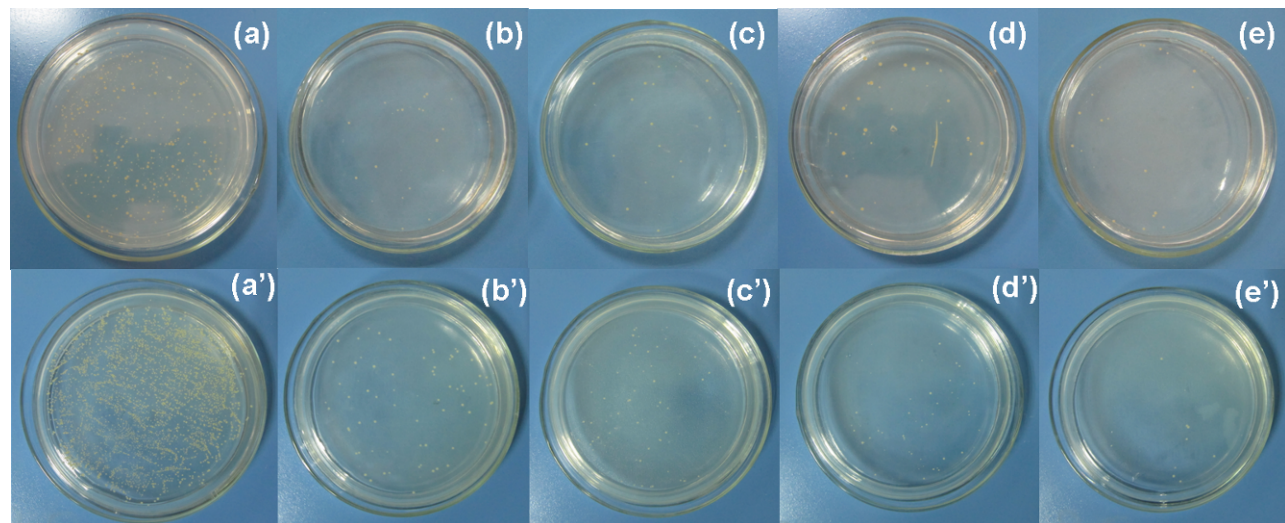


Fig. S7 Antibacterial test results using different amount of TiO_2 photocatalyst. For microsphere: (a) blank; (b) 0.5 layer; (c) 1 layer; (d) 1.5 layer; (e) 2 layer. (a')-(e') were the corresponding results for P25.

References

1. X. F. Tang, Y. G. Li, J. L. Chen, Y. D. Xu and W. J. Shen, *Micropor. Mesopor. Mat.*, 2007, **103**, 250-256.
2. K. Ishibashi, A. Fujishima, T. Watanabe and K. Hashimoto, *Electrochim. Commun.*, 2000, **2**, 207-210.